Catalysis Today 211 (2013) 104–108

Contents lists available at SciVerse ScienceDirect

Catalysis Today

journal homepage: www.elsevier.com/locate/cattod

Argon plasma reduced Pt nanocatalysts supported on carbon nanotube for aqueous phase benzyl alcohol oxidation

Chunmei Zhou [a], Hong Chen [a], Yibo Yan [a], Xinli Jia [a], Chang-jun Liu [b,**], Yanhui Yang [a,*]

[a] School of Chemical and Biomedical Engineering, Nanyang Technological University, Singapore 637459, Singapore
[b] Advanced Nanotechnology Center, School of Chemical Engineering and Technology, Tianjin University, Tianjin 300072, PR China

ARTICLE INFO

Article history:
Received 16 November 2012
Received in revised form 26 February 2013
Accepted 8 April 2013
Available online 13 May 2013

Keywords:
Plasma reduction
Platinum
Electrochemical measurement
Benzyl alcohol aerobic oxidation

ABSTRACT

Carbon nanotube supported Pt nano-catalyst was prepared by facile glow discharge plasma reduction operated at room temperature. The low-temperature plasma reduced Pt nanoparticles exhibited uniform size distribution and an average particle size of around 2.3 nm. Electrochemical measurements also proved that the plasma reduced Pt catalyst has remarkably higher active surface area comparing to the conventional hydrogen thermally reduced sample (3.6 nm in diameter). The plasma reduced Pt/CNT catalysts exhibited significantly higher conversion in benzyl alcohol aerobic oxidation compared to the hydrogen reduced Pt catalyst. Nonetheless, no obvious difference was found on the catalytic activity in terms of turn over frequency (TOF) between the plasma and hydrogen reduced Pt/CNT catalysts. Therefore, low temperature plasma reduction can effectively enhance Pt dispersion without changing its intrinsic catalytic property.

1. Introduction

Selective oxidation of benzyl alcohol to benzaldehyde is an important reaction in fine chemical industry, accounting for many products serving as the versatile intermediates in organic synthesis [1]. Supported noble metal catalysts, such as Pd [2,3], Pt [4], and Au [5], were extensively employed in this reaction due to their superior catalytic performances. The catalytic properties of these catalysts were intimately related to the metal particle size and the specific interaction between metal active sites and the supports [1,6], which may be largely changed by using different catalyst synthesis methods. Impregnation followed by hydrogen thermal reduction is a conventional method, and it has been adopted in numerous catalyst preparations. However, noble metal nanoparticles may agglomerate substantially under hydrogen thermal reduction at elevated temperature, resulting in the activity loss and weak interaction between metal particles and supports [7]. Chemical reductive deposition precipitation is another frequently used method, which requires reductive chemicals such as polyols [8], $NaBH_4$ [9], and urea [10].

Plasma reduction, the glow discharge in particular, has been demonstrated as a facile and green method in catalyst preparation, which is low energy consumption and free of chemical wastes. Glow discharge is a conventional non-thermal plasma that is characterized by its high electron temperature (10,000–100,000 K) and low gas temperature (near room temperature) [11]. Several metallic nanostructures have been reported based on this novel reduction technique, since the electrons in the glow discharge plasma can effectively reduce the metal ions into metallic phase at room temperature [12,13]. Wang et al. showed the platinum nanocatalyst supported on carbon black via plasma reduction, with a well-controlled particle size averaging at 1.43 nm for 20 wt.% Pt loading and 1.50 nm for 40 wt.% Pt loading [14]. Pt/Al_2O_3 [15] and Pt/TiO_2 [16] catalysts with high Pt dispersion were also prepared by this method. The synthesis of nanoporous Pt supported on nickel foam [17] and AuPd bimetallic nanoparticles confined in mesopores [18] were also reported via the Ar glow-discharge plasma reduction. Both catalysts exhibited excellent catalytic activities in electro-oxidation and solvent-free aerobic oxidation of alcohols. In this work, carbon nanotube supported Pt nano-catalyst was synthesized via the Ar glow-discharge plasma reduction method, and the catalytic properties were examined in the aqueous phase benzyl alcohol oxidation. The intrinsic catalytic properties of Pt were benchmarked against the Pt catalyst prepared by hydrogen thermoreduction.

2. Experimental

2.1. Materials

Multi-walled carbon nanotubes (MWCNT) was obtained from Cnano Technology Ltd. (purity: 97.1%, S_{BET}: 241 m^2/g, bulk density: 0.05 g/cm^3). HNO_3 (69%), H_2SO_4 (98%), KOH, H_2PtCl_4, ethylene

* Corresponding author. Tel.: +65 63168940; fax: +65 67947553.
** Corresponding author. Tel.: +86 22 27406490; fax: +86 22 27406490.
E-mail addresses: ughg_cjl@yahoo.com (C.-j. Liu), yhyang@ntu.edu.sg (Y. Yang).

0920-5861/$ – see front matter © 2013 Elsevier B.V. All rights reserved.
http://dx.doi.org/10.1016/j.cattod.2013.04.006

glycol (EG), benzyl alcohol (98%), benzaldehyde (98%) and benzalacide (98%) were provided by Sigma–Aldrich. All chemicals were used as received without further purification.

2.2. Catalyst preparation

The pristine MWCNT was pretreated with concentrated HNO_3 at 140 °C for 2 h to remove the amorphous carbonaceous and metallic impurities, as well as to introduce surface oxygen functional groups for anchoring metal precursors. To deposit Pt precursors onto the functionalized CNT, 0.5 g of CNT was immersed in 7.2 ml of H_2PtCl_6 solution (20 mg/ml), then dried at 373 K in vacuum (Pt loading of 5 wt.%). 0.5 g of dried sample was loaded onto a quartz boat and placed in a quartz tube with two stainless steel electrodes. The plasma was introduced to reduce the Pt precursors following the procedures reported in the previous work [18,19]. The entire process was carried out at room temperatures. After 8 plasma treatment cycles (with 10 min per cycle), the obtained sample was denoted as Pt/CNT-plasma. For the purpose of comparison, H_2PtCl_6 impregnated CNT was dried under ambient condition and reduced by conventional hydrogen thermal reduction at 400 °C for 2 h (5% H_2/Ar atmosphere), the obtained sample was denoted as Pt/CNT-IMP.

2.3. Catalyst characterizations

Metal loadings were confirmed by inductively coupled plasma (ICP, AA6800) measurement, hydrofluoric acid (40%) was employed to dissolve the samples. X-ray diffraction (XRD) patterns were recorded on a Bruker AXS D8Focus diffractometer using a Ni filtered Cu Kα radiation (λ = 0.154 nm), operated at 40 kV and 40 mA. XRD data were collected between 30° and 80° (2 theta) with a resolution of 0.02° (2 theta). Particle sizes and size distributions of Pt were observed by transmission electron microscopy (TEM, Philips Tecnai G2 F20, operated at 200 kV). The samples were suspended in acetone and dried on holey carbon-coated Cu grids. Electrochemical properties of the samples were measured by voltammetries on an Autolab PGSTAT302 potentiostat. All the electrochemical performance tests were carried out at room temperature (25 °C) in a rotating disk electrode system. The working electrode was prepared by dropping 40 μl of the catalyst ink onto a glassy carbon electrode. The ink was prepared by ultrasonically mixing 2 mg of catalyst sample with 1 ml of 0.025 wt.% Nafion in deionized water solution. Pt foil and Ag/AgCl electrode (+0.197 V vs. NHE) were used as the counter and reference electrodes, respectively. The cyclic voltammograms were first recorded in nitrogen purged 0.1 M KOH at a scan rate of 50 mV/s until reproducible voltammograms were obtained. For the electrochemical active surface area (EAS) measurement, the average Coulombic charge (Q_H) of hydrogen adsorption and hydrogen desorption was used to calculate the Pt EAS of the electrodes, using the equation EAS = $Q_H/210\ (\mu C/cm^2)/w$, in which 'w' represents the content of Pt in the catalysts [20]. Oxygen electro-reduction was measured in 0.1 M KOH saturated with oxygen by liner potential sweep at 10 mV/s. Benzyl alcohol electro-oxidation was measured in 0.2 M benzyl alcohol with 0.1 M KOH as electrolyte at 50 mV/s.

2.4. Catalytic reaction

The selective oxidation of benzyl alcohol (as well as 4-methylbenzyl alcohol and 4-nitrobenzyl alcohol) was carried out in a bath-type reactor operated under atmospheric conditions. Alcohol (1 mmol), deionized water (50 ml), and catalyst (4 mg, 0.001 mmol of Pt) were added into a three-necked glass flask, stirred continuously (1200 rpm) and heated to 75 °C in an oil bath. The temperature was controlled by a thermocouple, and a reflux condenser was used to condense the vapor of products. Oxygen flow (25 ml/min) was bubbled into the mixture to initiate the reaction. After the given reaction time, the catalyst powder was filtered off and the reactant and product were extracted using toluene (10 ml) for three times. The supernatant (mixture of residual reactant, product) was analyzed using an Agilent gas chromatograph 6890 equipped with a HP-5 capillary column (30 m long and 0.32 mm in diameter, packed with silica-based supel cosil), and flame ionization detector (FID). Dodecane was the internal standard. The turnover frequency (TOF) was defined as the number of benzyl alcohol (BA) converted over one surface-active Pt atom per hour:

$$\text{TOF}\ \ (h^{-1}) = \frac{M_{BA} \cdot X}{M_{Pt} \cdot D \cdot t}$$

where M_{BA} and M_{Pt} are the amount of BA and Pt in feed (mol) respectively, X is the conversion of BA, D is the Pt dispersion calculated using electrochemical method, and t is the reaction time (h).

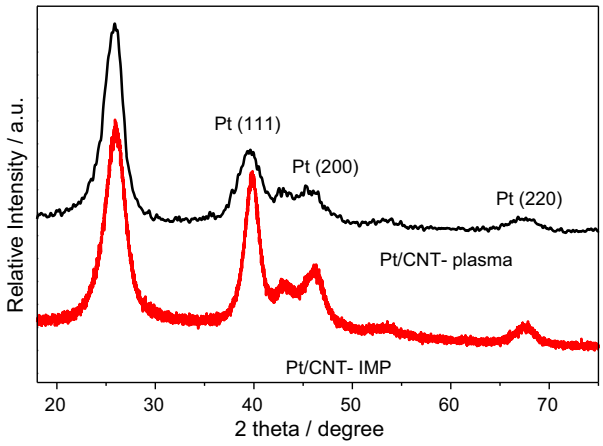

Fig. 1. XRD patterns of Pt/CNT-plasma and Pt/CNT-IMP catalysts.

3. Results and discussion

3.1. Characterization of catalysts

The XRD patterns for Pt/CNT-plasma and Pt/CNT-IMP (Fig. 1) show reflections at $2\theta = 39.8°$, 46.4° and 67.8°, ascribing to Pt(1 1 1), Pt(2 0 0) and Pt(2 2 0), respectively, which present the typical characteristics of crystalline Pt fcc pattern (PDF#04-0802). Half peak width of Pt reflections for Pt/CNT-plasma is remarkably wider than that of Pt/CNT-IMP, indicating the smaller average particle size for Pt/CNT-plasma. The particle sizes calculated from Pt(1 1 1) diffraction peak based on Scherrer's equation (as listed in Table 1) is 2.1 nm for Pt/CNT-plasma and 3.2 nm for Pt/CNT-IMP. TEM images of Pt/CNT-plasma and Pt/CNT-IMP are shown in Fig. 2. Pt is found uniformly dispersed on the surface of CNT for Pt/CNT-plasma, with an average particle size of 2.3 nm. For Pt/CNT-IMP, agglomerations of Pt particles obviously occur, and the average particle size of Pt is 3.6 nm. The TEM observations are well accord with the XRD results, and both characterizations prove that plasma reduction results in highly dispersed Pt nanoparticles, which may be due to the low temperature, while hydrogen thermal reduction leads to the agglomeration of Pt particles at high temperature. High-resolution TEM images (inset of Fig. 2) of Pt nanoparticles for both of Pt/CNT-plasma and Pt/CNT-IMP show the same lattice spacing of Pt(1 1 1) (approximately 0.228 nm), implying the similar electronic structures/properties of these two Pt catalysts.

To further characterize the catalysts and probe the electronic properties of Pt nanoparticles over these two catalysts, the

Table 1
Properties and catalytic performances of Pt/CNT-plasma and Pt/CNT-IMP catalysts.

Catalysts	D[a] (nm)	EAS[b] (m^2/g)	I_f[c] (A/g_{Pt})	Conversion[d] (%)	Selectivity[e] (%)	TOF[f] (h^{-1})
Pt/CNT-plasma	2.1	75.2	638.5	13.2	88.7	1234.9
Pt/CNT-IMP	3.2	36.6	309.4	6.4	87.9	1235.1

[a] Particle sizes calculated from XRD patterns of Pt(1 1 1) based on Scherrer's equation.
[b] EAS areas deduced from hydrogen adsorption of Fig. 3a.
[c] Max peak current measured from electro-oxidation of benzyl alcohol of Fig. 3b.
[d] Conversion of benzyl alcohol under the aerobic conditions of: benzyl alcohol 3 mmol, deionized water 15 ml,catalyst 12 mg, $T = 75\ ^{\circ}C$, $t = 1$ h, O_2 flow rate 25 ml/min.
[e] Selectivity to benzaldehyde in the aerobic oxidation of benzyl alcohol.
[f] TOF is defined as the number of converted benzyl alcohol molecules in 1 h over one active site.

electrochemical measurements were carried out and the results are shown in Fig. 3a. CV curves for both Pt/CNT-plasma and Pt/CNT-IMP display distinct hydrogen desorption/adsorption peaks in the potential range from −1.0 to −0.6 V. The hydrogen peak area of Pt/CNT-plasma is significantly larger than that of Pt/CNT-IMP, this and the calculations (listed in Table 1) together conform that the EAS of Pt/CNT-plasma (75.2 m^2/g) is much larger than that of Pt/CNT-IMP (36.6 m^2/g). The electro-oxidations of benzyl alcohol are conducted in 0.2 M of benzyl alcohol (in 0.1 M KOH aqueous solution), and their CV curves are depicted in Fig. 3b. Two oxidation peaks for benzyl alcohol electro-oxidation are observed for both catalysts. The first peak (−0.10 V) is ascribed to the oxidation of benzyl alcohol to benzaldehyde, and the second peak (0.25 V) is due to the deep oxidation of benzaldehyde to benzalacide [4]. The current for first oxidation peak on Pt/CNT-plasma is about two times larger than Pt/CNT-IMP, indicating that Pt/CNT-plasma is more efficient on activation of benzyl alcohol than Pt/CNT-IMP due to the high dispersion of Pt.

3.2. Catalytic performance of catalysts

Table 1 lists the catalytic performances of Pt/CNT-plasma and Pt/CNT-IMP in aerobic oxidation of benzyl alcohol in aqueous solutions. The benzyl alcohol conversion over Pt/CNT-plasma catalyst is nearly doubled as compared to Pt/CNT-IMP when the reaction time is 1 h, while the selectivity toward benzaldehyde over these two catalysts is similar. The time course duration of catalysts performance in benzyl alcohol oxidation is shown in Fig. 4. Both catalysts show stable activity, and the benzyl alcohol conversions monotonically increase as the reaction proceeds. After reacting for 5 h, only 16% conversion can be achieved over Pt/CNT-IMP while the conversion of Pt/CNT-plasma is about 30%. Compared to Pt/CNT-IMP,

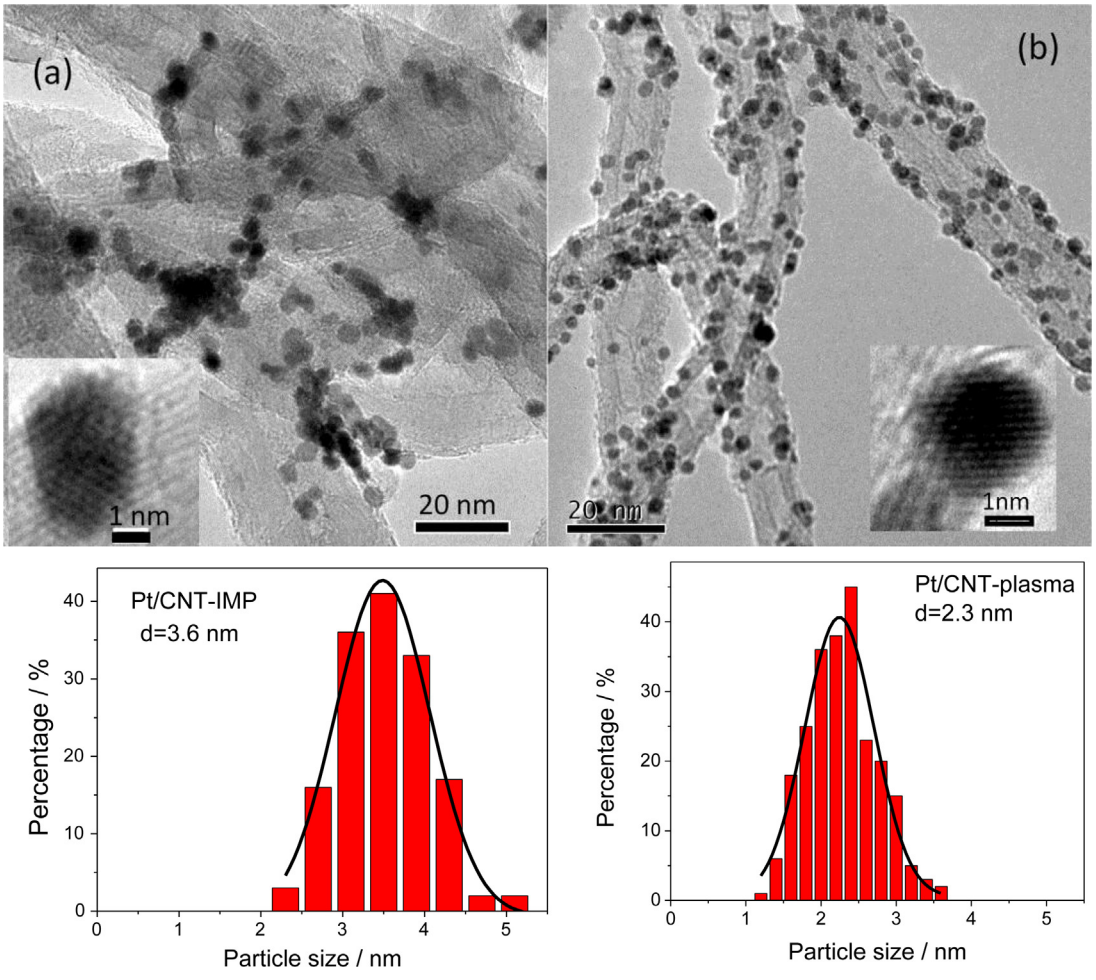

Fig. 2. TEM images and particle size distribution of Pt/CNT-IMP (a) and Pt/CNT-plasma (b).

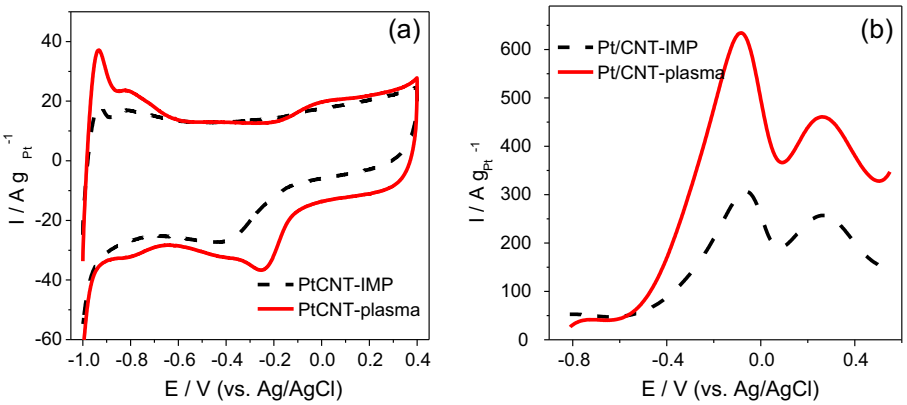

Fig. 3. Cyclic voltammograms of catalysts in 0.1 M KOH (a) and in 0.1 M KOH + 0.2 M benzyl alcohol (b).

Pt/CNT-plasma exhibits slightly faster deactivation rate, which may due to the remarkably higher catalytic conversion.

For both Pt/CNT-IMP and Pt/CNT-plasma catalysts, the catalytic activities, represented by TOFs, decrease with reaction time. Interestingly, the activities of Pt nanoparticles over these two catalysts are identical as demonstrated by the same TOFs. It conforms that the improved conversion for Pt/CNT-plasma is due to its high dispersion and surface area of Pt. Interestingly, different from the reported results that catalytic activity of noble metal nanoparticles in the aerobic oxidation of benzyl alcohol significantly depends on the particle size [21], no observable size effect was found in this study, at least, over these two catalysts. One of the plausible explanations to the inconsistency is the measurement of Pt dispersions which would affect the TOF results. In the above-mentioned results, the dispersions were measured by CO chemisorptions or calculated using Pd dispersion = 1.12/diameter of Pd particle (from TEM, nm). Nonetheless, the Pt dispersions were calculated by electrochemical absorption of H_2 and CO in this study. To further address this issue, alcohol substrates with different electron densities including 4-mthylbenzyl alcohol and 4-nitrobenzyl alcohol were introduced as probes to examine the catalytic activities of Pt/CNT-IMP and Pt/CNT-plasma, and the results are shown in Fig. 5. The conversions over Pt/CNT-plasma are constantly higher than Pt/CNT-IMP for different aromatic alcohols. Compared to benzyl alcohol, 4-mthylbenzyl alcohol shows a higher conversion, and 4-nitrobenzyl alcohol shows a lower conversion over both Pt/CNT-plasma and Pt/CNT-IMP catalysts. Both catalysts show higher catalytic activity for substituted aromatic alcohols containing electron-donating group (—CH_3) than those containing electro-withdrawing group (—NO_2) [2], implying that the electronic effect and intrinsic

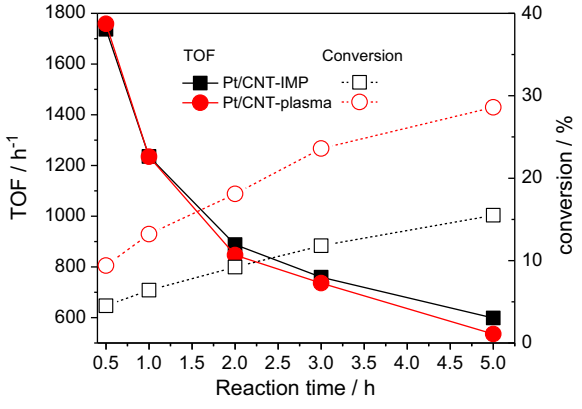

Fig. 4. Time course of catalysts for benzyl alcohol oxidation (conditions: benzyl alcohol 3 mmol, deionized water 15 ml, T = 75 °C, t = 0.25–5 h, O_2 flow rate 25 ml/min).

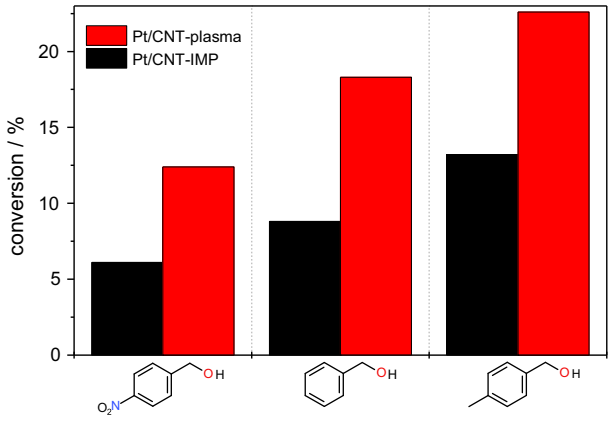

Fig. 5. Conversions of different aromatic alcohol substrates (conditions: alcohol 1 mmol, deionized water 50 ml, catalyst 4 mg (0.001 mmol Pt), O_2 flow rate 25 ml/min, T = 75 °C, t = 2 h).

properties of Pt nanoparticles over these two catalysts are the same. However, based on the previously reported mechanism for Ar glow-discharge plasma reduction of metal structures [22], the high-energy species generated by plasma, such as electrons and ions, should have directly reduce the metal ions through a recombination process, which would probably afford different Pt atomic arrangements as compare to the high temperature hydrogen reduced Pt

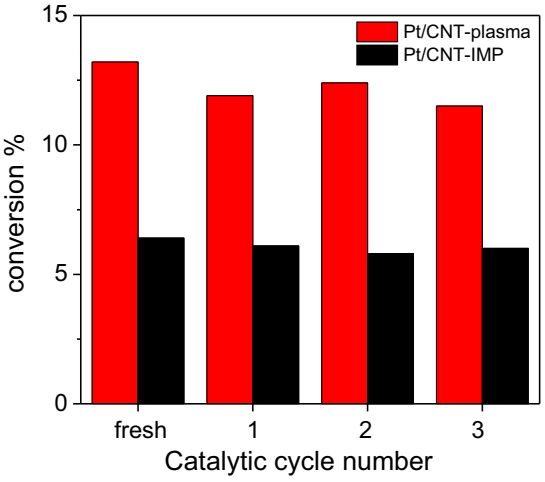

Fig. 6. Recycle tests for Pt/CNT-plasma and Pt/CNT-IMP in aerobic oxidation of benzyl alcohol (conditions: benzyl alcohol 3 mmol, deionized water 15 ml, T = 75 °C, t = 1 h for each cycle, O_2 flow rate 25 ml/min).

particles. A reasonable explanation for the disagreement between reported mechanism and this study is that the catalyst after plasma reduction may be unstable and has undergone the passivation after exposing to air and moisture.

Recycle performances were also studied and showed in Fig. 6. Both catalysts can be recycled for several times while the activities are retained. Less than 15% loss of conversion after 3 times recycle reactions is observed. In accordance with the reaction time course duration results, Pt/CNT-plasma exhibits slightly poorer stability than Pt/CNT-IMP in the recycle tests, which may due to the agglomeration of small Pt nanoparticles.

4. Conclusion

Argon glow discharge plasma reduction as a facile and green method was employed to fabricate the carbon nanotube supported Pt nano-catalyst. Pt nanoparticles reduced under Ar plasma at low temperature uniformly dispersed on the surfaces of CNT, possessing large accessible surface areas and enhanced catalytic conversion toward the selective oxidation of alcohols in aqueous solutions. The prepared catalyst can be recycled for several times without substantially losing the activity. Compared to the Pt catalyst reduced under hydrogen at high temperature, Pt/CNT-plasma showed almost identical catalytic activity (indexed by TOF) in the aerobic oxidation, which may due to the similar intrinsic properties of Pt nanoparticles prepared under two different methods.

Acknowledgments

This study is funded by the Singapore Agency for Science, Technology and Research (A*STAR, SERC Grant No. 102 101 0020) and the National Natural Science Foundation of China (Grant No. 20990223) and 111 Project of Ministry of Education of China (Grant No. B06006).

References

[1] D.I. Enache, J.K. Edwards, P. Landon, B. Solsona-Espriu, A.F. Carley, A.A. Herzing, M. Watanabe, C.J. Kiely, D.W. Knight, G.J. Hutchings, Science 311 (2006) 362.
[2] Y.T. Chen, Z. Guo, T. Chen, Y.H. Yang, Journal of Catalysis 275 (2010) 11.
[3] F.M. McKenna, R.P.K. Wells, J.A. Anderson, Chemical Communications 47 (2011) 2351.
[4] C.M. Zhou, Y.T. Chen, Z. Guo, X. Wang, Y.H. Yang, Chemical Communications 47 (2011) 7473.
[5] P. Haider, J.D. Grunwaldt, R. Seidel, A. Baiker, Journal of Catalysis 250 (2007) 313.
[6] P.J. Miedziak, Z.R. Tang, T.E. Davies, D.I. Enache, J.K. Bartley, A.F. Carley, A.A. Herzing, C.J. Kiely, S.H. Taylor, G.J. Hutchings, Journal of Materials Chemistry 19 (2009) 8619.
[7] Z. Guo, Y.T. Chen, L.S. Li, X.M. Wang, G.L. Haller, Y.H. Yang, Journal of Catalysis 276 (2010) 314.
[8] J.H. Bitter, A.J. Plomp, D.M.P. van Asten, A.M.J. van der Eerden, P. Maki-Arvela, D.Y. Murzin, K.P. de Jong, Journal of Catalysis 263 (2009) 146.
[9] P. Kim, J.B. Joo, W. Kim, J. Kim, I.K. Song, J. Yi, Journal of Power Sources 160 (2006) 987.
[10] W.J. Yan, Y.T. Chen, Y.H. Yang, T. Chen, Catalysis Today 174 (2011) 127.
[11] C.J. Liu, J.J. Zou, K.L. Yu, D.G. Cheng, Y. Han, J. Zhan, C. Ratanatawanate, B.W.L. Jang, Pure and Applied Chemistry 78 (2006) 1227.
[12] Z.J. Wang, Y.B. Xie, C.J. Liu, Journal of Physical Chemistry C 112 (2008) 19818.
[13] J.J. Zou, Y.P. Zhang, C.J. Liu, Langmuir 22 (2006) 11388.
[14] Z. Wang, C.J. Liu, G.L. Zhang, Catalysis Communications 10 (2009) 959.
[15] X.L. Zhu, P.P. Huo, Y.P. Zhang, C.J. Liu, Industrial and Engineering Chemistry Research 45 (2006) 8604.
[16] J.J. Zou, C.J. Liu, K.L. Yu, D.G. Cheng, Y.P. Zhang, F. He, H.Y. Du, L. Cui, Chemical Physics Letters 400 (2004) 520.
[17] C.M. Zhou, X. Wang, X.L. Jia, H.P. Wang, C.J. Liu, Y.H. Yang, Electrochemistry Communications 18 (2012) 33.
[18] Y.T. Chen, H.P. Wang, C.J. Liu, Z.Y. Zeng, H. Zhang, C.M. Zhou, X.L. Jia, Y.H. Yang, Journal of Catalysis 289 (2012) 105.
[19] H.P. Wang, C.J. Liu, Applied Catalysis B: Environmental 106 (2011) 672.
[20] A. Pozio, M. De Francesco, A. Cemmi, F. Cardellini, L. Giorgi, Journal of Power Sources 105 (2002) 13.
[21] Q.H. Zhang, W.P. Deng, Y. Wang, Chemical Communications 47 (2011) 9275.
[22] X. Liang, C.J. Liu, P. Kuai, Green Chemistry 10 (2008) 1318.